Extended Abstracts of the 2012 International Conference on Solid State Devices and Materials, Kyoto, 2012, pp174-175

Polycrystalline ZnO Mott-barrier diodes

Zi-Jheng Liu, Hsin-Wei Huang, Jon-Yiew Gan, and Tri-Rung Yew

Department of Materials Science and Engineering, National Tsing-Hua University, Hsinchu, Taiwan 30013, R.O.C
Phone: +886-3-571-5131 ext. 33853, Fax: +886-3-575-1979, E-mail: d9731832@oz.nthu.edu.tw

1. Introduction

A Mott barrier is a metal-semiconductor junction in which the semiconductor layer is intrinsic (or very lightly doped) and much narrower than its required depletion width [1, 2]. The structure can improve the RC time delay and burnout capability of a Schottky diode [3]. So far, Mott-barrier diodes have been mainly made of epitaxial single-crystal Si or GaAs [1]. However, their complex and high-temperature fabrication is difficult to be compatible with future device applications, such as three-dimensional memory arrays and flexible electronic circuits. This study reports the development of polycrystalline ZnO Mott-barrier diodes using a room-temperature sputtering process.

2. Experiments

We designed and fabricated Mott-barrier diodes in two forms of Pt/ZnO/ZnO:Al/Pt- and Pt/ZnO:Al/ZnO/Pt-stackd structures, as shown in Fig. 1. The two structures were fabricated on Pt/Ti/SiO_2/Si substrates at room temperature by RF magnetron sputtering. The thickness of ZnO and ZnO:Al thin films were controlled to approximately 15 nm and 20 nm, respectively. Finally, Pt top electrodes were sputter deposited with a thickness of 100 nm and a diameter of 70 μm, defining the diode area. In the electrical measurements, the voltage was applied on the top electrode, whereas the bottom electrode was ground.

3. Results and Discussion

Fig. 2 shows the grazing-incidence X-ray diffraction (XRD) patterns of ZnO/Pt, ZnO:Al/Pt, ZnO/ZnO:Al/Pt, and ZnO:Al/ZnO/Pt stacks. To analyze the crystallinity of polycrystalline ZnO-based films, their peak intensities were utilized as the comparison basis (the inset in Fig. 1). The crystallinity of ZnO thin films on ZnO:Al/Pt was higher than that on Pt. The similar phenomenon also appeared in the comparison of ZnO:Al thin films grown on ZnO/Pt and Pt. This reveals that the coherent growth can promote thin-film crystallization.

Fig. 3(a) shows the current density-voltage (*J*-*V*) characteristics. The Pt/ZnO/ZnO:Al/Pt diodes exhibited poor rectifying behaviors with a maximum rectification ratio of 4. In contrast, the Pt/ZnO:Al/ZnO/Pt diodes performed good rectifying characteristics with a maximum rectification ratio of 4.7×10^4, a forward current density of 1.6×10^3 A/cm^2 at 2 V, a diode factor of 2.3, and a turn-on voltage of ~1 V. The performance difference between the two structures could be attributed to the effect of surface chemical states and thin-film crystallization.

Fig. 3(b) shows the capacitance-voltage (*C*-*V*) characteristics. The capacitance of Pt/ZnO:Al/ZnO/Pt diodes was almost fixed under a reverse bias. This suggests that the depletion region was limited in the ZnO layer and difficult to be extended to the ZnO:Al layer, which is consistent with the Mott-barrier model. However, the high leakage current under a forward bias led to a roll-off in the measured capacitance when the applied voltage was higher than 0.9 V. The dielectric constant (κ) of the ZnO films extracted from the capacitance at V=0 was ~10.6, which is similar to values reported in previous literatures [4]. The capacitance decrease appeared in both forward-bias and reverse-bias regions for the Pt/ZnO/ZnO:Al/Pt diodes because high leakage current occurred in the both regions.

To analyze the barrier height at the ZnO/Pt junctions of the Pt/ZnO:Al/ZnO/Pt diodes, the reverse *J*-*V* curves were measured from 25 to 105 ^{o}C. Fig. 4 shows the Richardson plot of ln(J/V) versus 1000/T. The barrier height under different voltage bias can be calculated by thermionic emission fitting. The barrier height of ZnO/Pt interfaces at zero bias was estimated to be ~0.5 eV by linear extrapolation.

Regarding practical device operation, the transient behaviors and reliability under pulse stress are key issues. Fig. 5(a) shows the input voltage pulse pattern (V_{in}) and corresponding current response. Applying a full-wave voltage pulse with amplitude of ±2 V and width of 1 μs caused a half-wave current response, demonstrating the desirable rectifying behavior. In addition, the turn-on and turn-off transition can be stabilized within 50 ns [Fig. 5(b)]. Fig. 6 demonstrates that the diode can retain stable rectification under a ±2-V and 1-μs pulse stress up to 10^{10} cycles.

4. Conclusion

This study proposes polycrystalline ZnO Mott-barrier diodes fabricated by room-temperature sputtering. The proposed diodes exhibit high rectifying ratio of 4.7×10^4, short switching time of < 50 ns, and stable rectification up to 10^{10} cycles under ±2 V pulse stress. The satisfactory characteristics demonstrate the potential for future device applications.

References

[1] S. M. Sze and K. K. Ng, *Physics of Semiconductor Devices* 3rd ed. New York: Wiley (2007) chap. 3.
[2] N. F. Mott, Proc. Cambridge Philos. Soc. **34** (1938) 568.
[3] M. McColl and M. F. Millea, Proc. IEEE **61** (1973) 499.
[4] R. Menon, K. Sreenivas, and V. Gupta, J. Appl. Phys. **103** (2008) 094903.

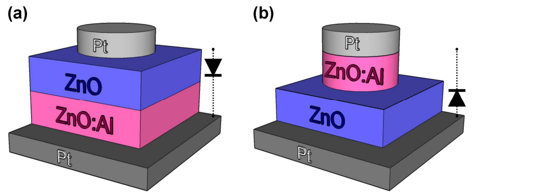

Fig. 1. Schematics of ZnO Mott-barrier diodes with (a) Pt/ZnO/ZnO:Al/Pt and (b) Pt/ZnO:Al/ZnO/Pt structures.

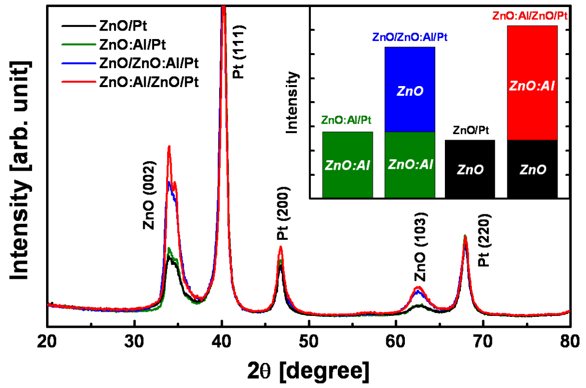

Fig. 2. Grazing-incidence XRD patterns of ZnO/Pt, ZnO:Al/Pt, ZnO/ZnO:Al/Pt, and ZnO:Al/ZnO/Pt stacks. The inset shows the ZnO peak intensities of the four stacks.

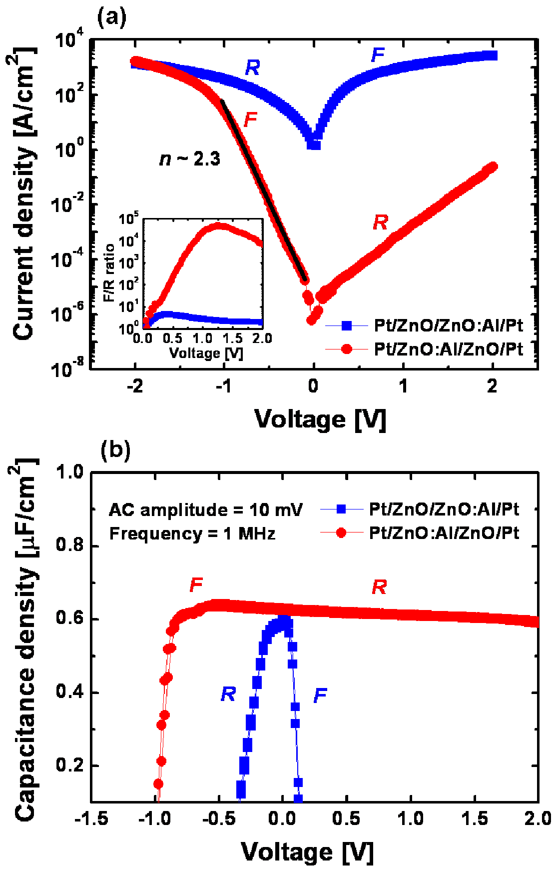

Fig. 3. (a) *J-V* and (b) *C-V* characteristics of Pt/ZnO/ZnO:Al/Pt and Pt/ZnO:Al/ZnO/Pt diodes. The notations of *F* and *R* represent the forward-bias and reverse-bias regions, respectively. The inset in (a) shows the *F*/*R* current ratio of the two diodes.

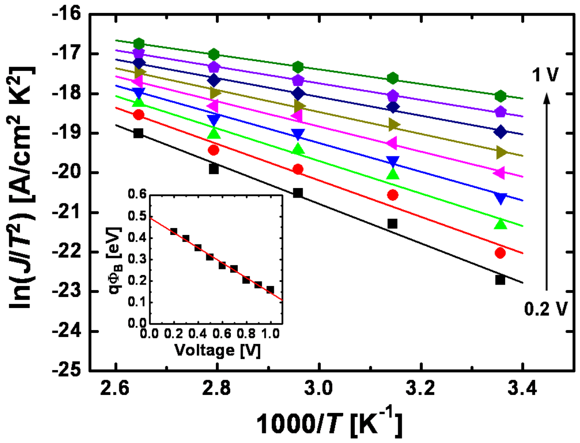

Fig. 4. Richardson plot of ln(J/T^2) versus 1000/T for the Pt/ZnO:Al/ZnO/Pt diode under reverse bias in the temperature range of 25-105 °C. The inset shows the ZnO/Pt barrier height as a function of applied voltage.

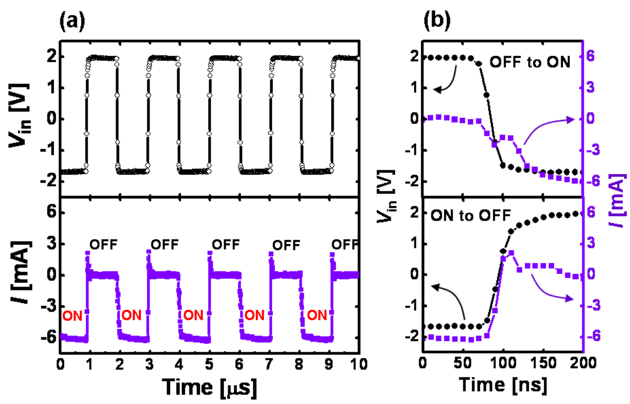

Fig. 5. (a) Input voltage pulse pattern (V_{in}) and corresponding current response. (b) Transient behaviors of turn-on and turn-off switching.

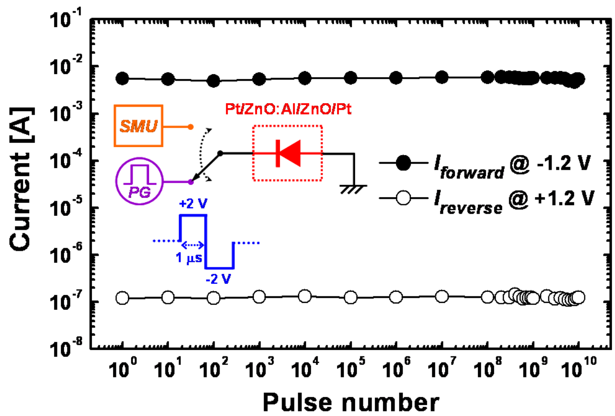

Fig. 6. Reliability test under ±2 V pulse stress up to 10^{10} cycles.